Journal of Southeast University (English Edition) Vol. 25, No. 1, pp. 89 – 93 Mar. 2009 ISSN 1003—7985

Ultimate negative bending-moment capacity of outer-plated steel-concrete continuous composite beams

Chen Lihua[1,2] Li Aiqun[1] Lou Yu[3] Li Peibin[3]

([1] School of Civil Engineering, Southeast University, Nanjing 210096, China)
([2] College of Civil and Architectural Engineering, Hefei University of Technology, Hefei 230009, China)
([3] China Electronics Engineering Design Institute, Beijing 100840, China)

Abstract: Static load tests and bearing capacity analyses are carried out for two outer-plated steel-concrete continuous composite beams. The load-deflection curve and the load-strain curve of specimens are obtained and analyzed. The test results indicate that effective cooperation can be achieved by the shear-resistant connection between the reinforcement in the negative moment area and the outer-plated steel beam, and the overall working performance of the composite beams is favorable. At the load-bearing limiting state, the plastic strain on the maximum negative and positive moment section becomes fully developed so as to form relatively ideal plastic hinges. With the increase in the reinforcement ratio, the moment-carrying capacity of the composite beams improves significantly, but the ductility of the beams and the rotation ability of the plastic hinges decrease. The formulae for calculating the limit bending capacity in the negative moment area of outer-plated steel-concrete composite beams are proposed based on the test data. The calculated results agree well with the test results.

Key words: outer-plated steel-concrete composite beam; continuous beam; negative moment; bending-moment bearing capacity

The steel-concrete composite beam is a beam derived from a suitable connection and cooperation between steel and concrete. The types of steel-concrete composite beams adopted at home and abroad are mostly the steel-concrete composite beam, the shaped steel-concrete composite beam, the prestressed steel-concrete composite beam and the outer-plated steel-concrete composite beam. The outer-plated steel-concrete composite beam under current study is usually formed by casting concrete in a thin-wall roll-formed shape steel bay, and the cooperation between steel and concrete is achieved by shear connecting elements. The outer-plated steel-concrete composite beam proposed in this paper adopts a U-shaped cross section as a beam rib formed by welding a thick steel bottom plate with a thin-wall steel web. The concrete is cast into the rib and the upper flange of the U-shaped section, then the outer-plated U-shaped steel beam and the concrete slab with a T-shaped section are joined together by the introversive upper flange of the U-shaped section as well as by the shear connecting elements[1]. This new type of composite beam has many advantages, such as the saving of steel, the enhancement of the local stability, the global stability, the fire resistance of the steel components, the better performance of carrying the negative bending moment, the easier control of the relative slide between steel components and concrete, etc. Under the conditions of the same section configuration, loading, and supporting, the continuous composite beams are more advantageous than the simply-supported ones due to their better load-carrying performance, distinctly enhanced integrity, and the antiseismic behavior of the floor system. Therefore, the continuous composite beams are more widely used in engineering. Herein, in order to investigate the section capacity of carrying the negative bending moment for this new type of composite beams, static load tests are conducted for two outer-plated steel-concrete continuous composite beams.

Received 2008-05-29.

Biographies: Chen Lihua (1972—), female, doctor; Li Aiqun (corresponding author), male, doctor, professor, aiqunli@sina.com.

Citation: Chen Lihua, Li Aiqun, Lou Yu, et al. Ultimate negative bending-moment capacity of outer-plated steel-concrete continuous composite beams [J]. Journal of Southeast University (English Edition), 2009, 25(1): 89 – 93.

1 Design and Fabrication of Specimens

Based on the previous researches of the simply-supported outer-plated steel-concrete composite beams made by our research group[2–3] and other domestic studies of steel-concrete continuous composite beams[4–9], two specimens of outer-plated steel-concrete continuous composite beams, numbered SBD1 and SBD2, are designed. The complete shear connection is adopted for these two tested beams, excluding the effects of slippage on the working performance of the tested beams. Two U-shaped outer-plated steel beams are designed with the same cross section, in which a 10 mm thick bottom plate and 4 mm thick side plates are used. The longitudinal steel bars put in the concrete flange slab in the regions of the negative bending moment are $7\underline{\phi}18$ and $9\underline{\phi}18$, respectively, for the two beams. Tab. 1 lists the material properties of the steel. The construction details of the specimens are shown in Fig. 1. In order to prevent the horizontal shear failure along the interfaces between the concrete flange slab and the U-shaped outer-plated steel beams, 56 cotters are welded on the flange of the beams and the HPB235 steel dowels with a diameter of 10 mm are arranged in the beams. The concrete strength of the specimens is obtained via the test of 10 cm cubes cured under the same conditions as the specimens. The commuted axial compressive strength of concrete f_c is 26.8 MPa.

Tab. 1 Material properties of steel specimens

Type	Thickness/mm	Diameter/mm	Yield strength f_y/MPa	Ultimate strength f_u/MPa	Elongation rate δ/%
Steel bar		10	340	480	28
		18	390	580	22
Steel plate	10		390	560	27
	4		260	360	38

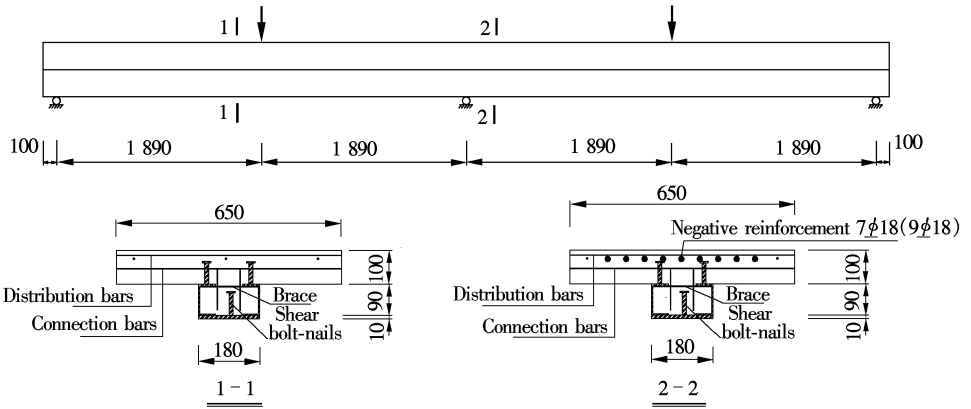

Fig. 1 Construction of composite beams SBD1, SBD2

2 Experimental Method

The two specimens are tested with one-point monotonic mid-span loading. 50-t oil jacks are settled in each mid-span with one oil circuit shared between two jacks to ensure the synchronous application of load. At the cross sections of each mid-span and intermediate supports, strain gauges are located on the concrete, the longitudinal steel bars and the outer-plated steel plates to observe the strain distribution of the sections with the maximum positive or negative moment. Displacement transducers and pressure transducers are also arranged to control the loading procedure and measure the mid-span deflections as well as the settlement and reaction of supports. The test data are collected by the Japanese TDS-303 data-collecting system. The loading mechanism is shown in Fig. 2.

Fig. 2 Loading mechanism

3 Data Analyses

3.1 Load-deflection curves

The measured relationships between the load and the mid-span deflection of the specimens are given in Fig. 3, in which SBD_L and SBD_R represent the measured mid-span deflections in the left and the right spans of specimens SBD1 and SBD2, respectively. It can be seen that the curves can be divided into three distinct stages (elasticity, elastoplasticity and plasticity), indicating a favorable ductility of the outer-plated steel-concrete composite beams. The characteristics of the loads are listed in Tab. 2, where P_{cr} represents the cracking load (the measured load when the first crack occurs on the surface of the concrete flange); P_y is the yielding load (the measured load when the intermediate support section or the mid-span section of the beams yields to form the first plastic hinge); P_u is the ultimate load (the greatest load when the failure of specimens occurs); δ_y and δ_u are the measured mid-span deflections corresponding to the loads P_y and P_u, respectively.

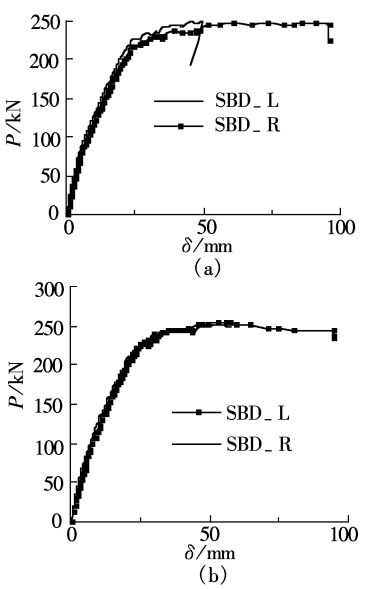

Fig. 3 Load-midspan deflection curves of specimens. (a) SBD1; (b) SBD2

Both the specimens span 3.78 m with a span-depth ratio of 18.9. Before the plastic hinge forms, the mid-span deflections are smaller than 1/200 of the beam span (18.90 mm), indicating a good integrity of the outer-plated steel-concrete continuous composite beams. In designing, higher span-depth ratios can be adopted to reduce the height of the beams and then to increase the clear height of the building.

Tab. 2 Experimental results of specimens

Specimen	P_{cr}/kN	M_{cr}/(kN·m)	P_y/kN	P_u/kN	δ_y/mm	δ_u/mm	δ_u/δ_y
SBD1	37.39	25.5	165.28	246.49	15.66	95.96	6.13
SBD2	37.92	27.8	172.67	253.75	16.15	87.07	5.39

3.2 Strain of steel beams and steel bars

The measured strain distribution on the support section of the continuous beam (beam SBD1) is shown in Fig. 4. During the elastic stage, the strain is almost linear along the height of the cross section. With the increase in loads and the strains descending of the neutral axis, the strain distribution along the section height of the outer-plated steel-concrete composite beam under the negative bending moment accords well with the plane cross-section assumption before the load reaches $0.9P_u$. The cooperation between the U-shaped steel beam and the concrete is favorable.

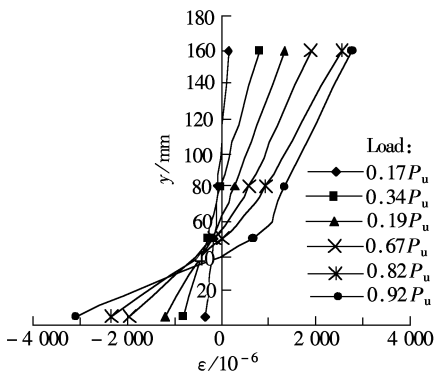

Fig. 4 Distribution of strain in cross section

The measured relationships between the loads and the strains of the longitudinal steel bars and the bottom plates of beams SBD1 and SBD2 are displayed in Fig. 5 and Fig. 6, respectively. Where S11, S21 and S31 denote three different steel bars within the same cross section; B1 and B2 are different positions on the same cross section of the bottom plate. Fig. 5 shows that if a suitable reinforcement ratio is provided, little distinction exists among the strains of different longitudinal steel bars on the same cross section with the effective flange width of concrete, from the elastic stage until the approach of the limit state of load-carrying capacity. The steel bars can fit well with the outer-plated steel beam, fully apply their tensile strength yields at failure of the beam.

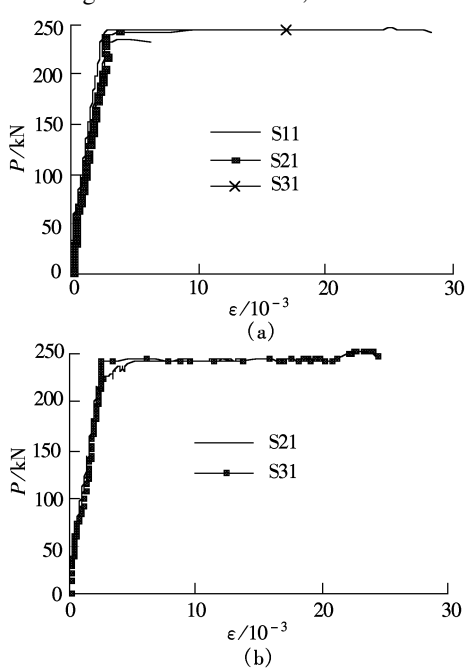

Fig. 5 Load-strain curves of steel bars in the negative moment area. (a) SBD1; (b) SBD2

From Fig. 6, it can be seen that the strains on the bottom plate of the U-shaped outer-plated steel beam change in consistence with each other, indicating the uniform stress state of the bottom plate. After the bottom plate yields under compression, the strains increase in a nonlinear trend. When reaching or approaching the ultimate load, the strains grow faster while little decrease in the load is observed. The plastic hinge formed by the support section displays a perfect rotation ability.

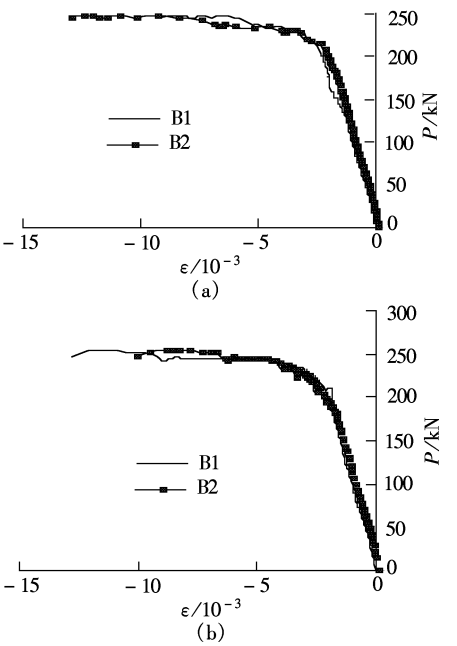

Fig. 6 Load-strain curves of outer-plated steel slabs in the negative moment area. (a) SBD1; (b) SBD2

4 Moment Carrying Capacity of Composite Beams under Negative Bending Moment

4.1 Basic assumption

1) A reliable connection exists between the outer-plated steel and the concrete. The tiny relative slide is ignored[1-3].

2) The section remains to be a plane; that is, the average strains of the steel and the concrete conform to the plane cross-section assumption from the beginning of loading until the failure.

3) Under the limit state, the concrete displays a rectangular distribution of its compressive stress and reaches its limit compressive strain. The effect of the concrete under tension is ignored.

4) Under the limit state, all the steel plates and steel bars yield, no matter whether they are in the tension area or in the compression area.

4.2 Ultimate moment carrying capacity under negative bending moment

Based on the above assumptions, the ultimate moment carrying capacities of the composite beams under the negative bending moment are analyzed and divided into the fol-

lowing two situations according to the location of the neutral axis.

1) The plastic neutral axis is located within the web of the steel beam; namely, the following condition is satisfied:

$$f_{sy}A_s < f_{by}A_b + f_{wy}A_w + 0.8f_c bh_w \tag{1}$$

The simplified stress distribution of the beam section is shown in Fig. 7(a). Then, according to the equilibrium of forces, we can obtain

$$f_{sy}A_s + 2f_{wy}t_w(h_w - x) = f_{by}A_b + 2f_{wy}t_w x + 0.8f_c bx \tag{2}$$

Thus the height of the real compression area of concrete x, which is the distance between the neutral axis and the internal surface of the bottom plate, becomes

$$x = \frac{f_{sy}A_s + f_{wy}A_w - f_{by}A_b}{0.8f_c b + 4f_{wy}t_w} \tag{3}$$

The ultimate moment carrying capacity of the composite beams is obtained by calculating the moment about the center of the bottom plate.

$$M_u = f_{sy}A_s\left(h_0 - \frac{t_b}{2}\right) + f_{wy}t_w(h_w - x)(h_w + t_b + x) - 0.4f_c bx(0.8x + t_b) + f_{wy}t_w x(x + t_b) \tag{4}$$

where A_b is the area of the bottom plate; A_w is the total area of the steel web; h_w and t_w are the height and thickness of the sideweb on one side, respectively; f_{by} and f_{wy} are the yield strengths of the bottom plate and web, respectively; b_f and h_f are the width and thickness of the concrete flange slab, respectively; f_c is the axial compressive strength of concrete; and M_u is the ultimate moment carrying capacity of the composite beam.

According to Eq. (3), if $x \geqslant 0$ (namely, the bottom plate of the outer-plated steel reaches yield under the ultimate state), the strength of the longitudinal steel bars inside the concrete flange slab should satisfy

$$f_{sy}A_s \geqslant f_{by}A_b - f_{wy}A_w \tag{5}$$

Otherwise, the strength of the bottom plate of the outer-plated steel cannot be fully achieved under the ultimate state. The outer-plated steel-concrete composite beam, which is difficult to reach local buckling of the steel, will cause a waste of material and a reduction in the load-bearing capacity in the negative bending moment area.

2) The plastic neutral axis is located within the concrete flange slab; namely, the following condition is satisfied:

$$f_{sy}A_s > f_{by}A_b + f_{wy}A_w + 0.8f_c bh_w \tag{6}$$

The simplified stress distribution of the beam section is shown in Fig. 7(b). According to the equilibrium of forces, we can obtain

$$f_{sy}A_s = f_{by}A_b + f_{wy}A_w + 0.8f_c bx \tag{7}$$

In Eq. (7), part of the compression effect of the concrete flange slab is ignored. Thus the height of the real compression area of the concrete should be

$$x = \frac{f_{sy}A_s - f_{by}A_b - f_{wy}A_w}{0.8f_c b} \tag{8}$$

The ultimate moment carrying capacity of the composite beams is

$$M_u = f_{sy}A_s(h_0 - t_b/2) - 0.5f_{wy}A_w(h_w + t_b) - 0.4f_c bx(0.8x + t_b) \tag{9}$$

A comparison between the tested data and the calculated results of the ultimate bending moment on the central support section is presented in Tab. 3. The data in the table illustrate that it is suitable to calculate the ultimate moment-carrying capacity of composite beams under the negative bending moment by the simplified plastic theory.

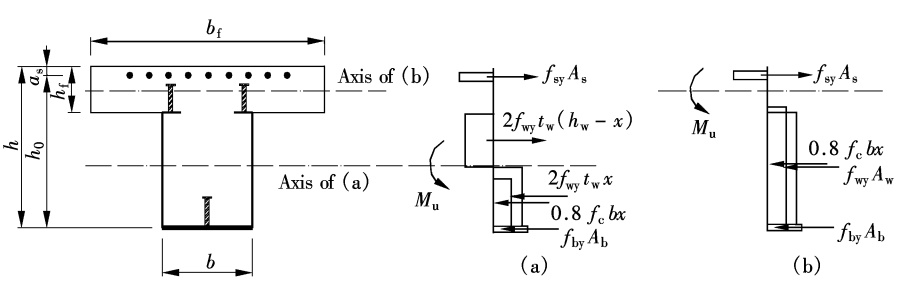

Fig. 7 The stress of the cross section of the specimens

Tab. 3 Comparison between the tested and calculated data of ultimate bending moment

Specimen	x/mm	Limit height of compression area/mm	Theoretical values M_c/(kN·m)	Tested values M_t/(kN·m)	M_c/M_t
SBD1	22.4	67.5	111.8	123.8	0.903
SBD2	47.1	67.5	140.2	152.96	0.917

5 Conclusions

1) By filling concrete into the U-shaped steel beams, the outer-plated steel-concrete composite beams can improve the local and global stability of the beams with satisfactory overall working performance.

2) If the reinforcement ratio is suitable, the steel bars with an effective flange width of concrete in the negative bending moment area can fit well with the outer-plated steel beam. The plastic hinge formed on the support section dis-

plays a perfect rotational ability.

3) The reinforcement ratio of the longitudinal steel bars is one of the primary factors that affects the working performance of the composite beams under the negative bending moment. With the increase in the reinforcement ratio, the moment-carrying capacity of the composite beams improves significantly, but the ductility of the beams and the rotational ability of the plastic hinges decrease.

4) A practical formula for calculating the ultimate moment-carrying capacity of the outer-plated steel-concrete composite beams in the negative moment area is presented. The theoretical results accord well with the test results.

References

[1] Chen Lihua. Experimental investigation on the new-type outer-plated steel-concrete continuous composite beams and joints[D]. Nanjing: School of Civil Engineering of Southeast University, 2006. (in Chinese)

[2] Du Derun, Li Aiqun, Chen Lihua. Experimental study on steel encased concrete composite beam[J]. *Building Structure*, 2007, **36**(4): 64 - 67. (in Chinese)

[3] Xiao Hui, Li Aiqun, Du Derun. Experimental study on ultimate flexural capacity of steel encased concrete composite beams[J]. *Journal of Southeast University*: *English Edition*, 2005, **21**(2): 191 - 196.

[4] Zhu Pinru, Gao Xiangdong, Wu Zhensheng. Research on plastic hinge behaviour and internal moment redistribution in steel concrete continuous composite beam[J]. *Journal of Building Structures*, 1990, **11**(6): 26 - 37. (in Chinese)

[5] Wang Ting, Nie Jianguo, Li Bingyi, et al. Study on ultimate flexural capacity of composite steel-concrete beams with profiled sheeting[J]. *Journal of Building Structures*, 2001, **22**(2): 61 - 65. (in Chinese)

[6] Oehlers D J, Nguyen N T, Ahmed M, et al. Partial interaction in composite steel and concrete beams with full shear connection[J]. *Journal of Constructional Steel Research*, 1997, **41**(2/3): 235 - 248.

[7] Fabbrocino G, Manfredi G, Cosenza E. Ductility of composite beams under negative bending: an equivalence index for reinforcing steel classification[J]. *Journal of Constructional Steel Research*, 2001, **57**(2): 185 - 202.

[8] Fabbrocino G, Manfredi G, Cosenza E. Analysis of continuous composite beams including partial interaction and bond [J]. *Journal of Structural Engineering*, 2000, **126**(12): 1288 - 1294.

[9] Manfredi G, Fabbrocino G, Cosenza E. Modeling of steel-concrete composite beams under negative bending[J]. *Journal of Engineering Mechanics*, 1999, **125**(6): 654 - 662.

外包钢-混凝土连续组合梁的负弯矩极限承载力

陈丽华[1,2] 李爱群[1] 娄 宇[3] 李培彬[3]

([1] 东南大学土木工程学院,南京 210096)

([2] 合肥工业大学土木建筑工程学院,合肥 230009)

([3] 中国电子工程设计院,北京 100840)

摘要:对2根外包钢-混凝土连续梁试件进行了静力加载实验研究与承载力分析. 测量并分析了试件的荷载-挠度及荷载-应变关系曲线. 结果表明:外包钢-混凝土组合梁负弯矩区钢筋和外包钢梁通过抗剪连接措施能有效地共同工作,整体工作性能良好. 在承载能力极限状态,负弯矩和正弯矩最大截面的塑性应变均充分发展,并形成比较理想的塑性铰. 随着配筋率的提高,组合梁受弯承载力明显提高,而延性和转动能力相应降低. 在试验数据基础上,给出了外包钢-混凝土组合梁在负弯矩区极限受弯承载力的计算公式,计算结果与实验结果吻合良好.

关键词:外包钢-混凝土组合梁;连续梁;负弯矩;受弯承载力

中图分类号:TU317.1